Molecular Biology of the Cell
Vol. 3, 621–631, June 1992

Calcium Pools Mobilized by Calcium or Inositol 1,4,5-Trisphosphate are Differentially Localized in Rat Heart and Brain

Ajay Verma*, David J. Hirsch, and Solomon H. Snyder

The Johns Hopkins University School of Medicine, Departments of Neuroscience, Pharmacology and Molecular Sciences, and Psychiatry, Baltimore, Maryland 21205

Submitted March 18, 1992; Accepted April 20, 1992

Calcium-induced calcium release (CICR) pools have been demonstrated in brain and heart microsomes biochemically and autoradiographically by the sensitivity of $^{45}Ca^{2+}$ accumulation to Mg^{2+}, ATP, ruthenium red, caffeine, and tetracaine. The CICR pool colocalizes with [^{3}H]ryanodine binding sites, supporting the notion that [^{3}H]ryanodine labels CICR pools. Sites of CICR pools in the brain contrast with those of inositol 1,4,5-trisphosphate (IP_3)-sensitive Ca^{2+} pools with reciprocal localizations between the two Ca^{2+} pools in several structures. Thus, in the hippocampus CA-1 is enriched in IP_3-sensitive Ca^{2+} pools, whereas CICR pools are highest in CA-3 and the dentate gyrus. The corpus striatum and cerebellum are enriched in IP_3 pools, whereas the medial septum and olfactory bulb have high CICR densities. In cardiac tissue, CICR is localized to atrial and ventricular muscle, whereas IP_3 pools are concentrated in coronary vessels and cardiac conduction fibers. The reciprocal enrichment of IP_3 and CICR Ca^{2+} pools implies differential regulation of Ca^{2+} homostasis in these tissues.

INTRODUCTION

The release of Ca^{2+} from sarcoplasmic reticulum (SR) has been extensively characterized in striated muscle, where initial release of Ca^{2+} is triggered by Ca^{2+} itself (Endo, 1977; Fabiato, 1983; Moutin and Dupont, 1988). This Ca^{2+}-induced Ca^{2+} release (CICR) process is facilitated by ATP and caffeine and inhibited by local anesthetics, ruthenium red, and magnesium (Johnson and Inesi, 1969; Smith *et al.*, 1986; Moutin and Dupont, 1988; Wimsatt *et al.*, 1990). The CICR process is localized in skeletal muscle to terminal cisternae, where it can be activated by the plant alkaloid ryanodine (Inui *et al.*, 1987; Fill and Coranado, 1988; Chu *et al.*, 1990). [^{3}H]Ryanodine has been employed to label the CICR channel, which has been purified to homogeneity and molecularly cloned (Inui *et al.*, 1987; Takeshima *et al.*, 1989; Kinya *et al.*, 1990). In neuronal tissues, endoplasmic reticulum (ER) Ca^{2+} release has been best characterized with inositol 1,4,5-trisphosphate (IP_3). IP_3 releases between 50 and 70% of the ER Ca^{2+} in brain tissue, glands, and smooth muscle (Berridge and Irvine, 1989), whereas regulation of the IP_3-resistant ER Ca^{2+} pools has been less clear. It has been suggested that CICR regulates the IP_3-insensitive ER Ca^{2+} pools of nonmuscle cells including neurons (Thayer *et al.*, 1988; Goldbeter *et al.*, 1990; Meldolesi *et al.*, 1990) and that CICR initiated with Ca^{2+} released by IP_3 accounts for oscillations of intracellular free Ca^{2+} (Berridge and Galione, 1988; Goldbeter *et al.*, 1990; Randriamampita *et al.*, 1991; Tsunoda, 1991).

[^{3}H]Ryanodine binding sites have been demonstrated in brain tissue of chick (Ellisman *et al.*, 1990), rabbit (McPherson and Campbell, 1990; McPherson *et al.*, 1991), and rat (Ashley, 1989; Lai *et al.*, 1990; Padua *et al.*, 1991; Zimanyi and Pessah, 1991), and evidence has been obtained in various cultured neuronal cells for the release of Ca^{2+} by Ca^{2+} and for the effects of CICR modulators (Ashley, 1989; Thayer *et al.*, 1988; Mekhail-Ishak *et al.*, 1987; Lavoie *et al.*, 1986; Holliday *et al.*, 1991). The relationship of CICR to the IP_3-sensitive and IP_3-insensitive Ca^{2+} pools is unclear. In avian cerebellar Purkinje neurons, both IP_3 and ryanodine receptors coexist within the same cell's ER membranes both in overlapping and nonoverlapping intracellular structures (Walton *et al.*, 1991). The relative roles of these intracellular Ca^{2+} channels in regulating calcium pools in other brain regions or in mammalian brain is unknown.

* Present address: Walter Reed Army Medical Center, Department of Neurology, Washington, D.C.

We have shown that accumulation of $^{45}Ca^{2+}$ and its release by IP_3 vary markedly in different rat brain regions (Verma *et al.*, 1990a,b). In the present study we directly demonstrate IP_3-, Ca^{2+}-, and caffeine-induced Ca^{2+} flux in rat brain and heart microsomes and, by autoradiography, show discrete localizations of the apparent CICR pool of ER Ca^{2+} differing from IP_3-sensitive pools of Ca^{2+}. We also show pharmacological differences between brain and heart CICR processes.

MATERIALS AND METHODS

Tissue Preparation

Male Sprague-Dawley rats were decapitated; brains and hearts were rapidly removed and placed in ice-cold homogenization buffer (20 mM) *N*-2-hydroxyethylpiperazine-*N'*-2 ethanesulfonic acid (HEPES) [pH 7.35 with potassium hydroxide (KOH)], 0.25 M sucrose, 100 μM EDTA, and protease inhibitors. Protease inhibitors were phenylmethanesulphonylfloride (100 mg/ml), Nα-p-tosylarginine methylester (10 mg/ml), leupeptin (5 mg/ml), and aprotinin (5 mg/ml). Microsomes were prepared by mincing hearts with a scissors in 10 vol of ice-cold homogenization buffer (wt/vol) and were then homogenized with a polytron homogenizer (Wheaton, Millville, NJ) at speed 5 for 15 s ×3. Brains were homogenized in 10 vol (wt/vol) with a glass Teflon homogenizer at speed 5 using five up and down strokes. Homogenates were centrifuged at 10 000 × *g* with a Sorvall SS-34 rotor in a Beckman centrifuge for 15 min at 4°C. The supernatants were then centrifuged at 100 000 × *g* in a Beckman LS-80M ultracentrifuge for 60 min at 4°C. The pellets were then resuspended with a glass Teflon homogenizer in ice-cold homogenization buffer without enzyme inhibitors or EDTA to a protein concentration of 5 mg/ml and stored at −70°C. Protein was determined with the bicinchoninic acid protein assay reagent (Pierce, Rockford, IL) with bovine serum albumin as a standard.

Fresh frozen cryostat sections were obtained by rapidly freezing organs in tissue-Tek embedding medium (Miles, Naperville, IL) and mounting on microtome chucks. Cryostat sections (20 μM) were thaw mounted onto slides coated with 0.5% gelatin/0.05% chrome alum and stored at −70°C.

Ca^{2+} Uptake Assay

$^{45}Ca^{2+}$ uptake into microsomes was studied in 20 mM HEPES, 75 mM potassium phosphate (pH 7.3 with KOH), 3% polyethylene glycol (PEG, average molecular weight 8000), 10 mM phosphocreatine, 10 U/ml creatine phosphokinase, 1 mM total $CaCl_2$, 0.2 μCi/ml $^{45}Ca^{2+}$, 4 mM 1,4-dithiothreitol (DTT), 5 mM sodium azide, and indicated additions. Free calcium concentrations were adjusted to desired levels with EGTA with the use of a Ca^{2+}-sensitive electrode (Orion, Charlestown, MA). ATP and Mg^{2+} were added at 2 mM each except where indicated. Microsomes were added to a final protein concentration of 100 μg/ml to initiate $^{45}Ca^{2+}$ uptake at 37°C routinely for 15 min in a total volume of 0.5 ml. Assays were terminated by rapid filtration with 0.3% polyethyleneimine-coated 0.45-μM millipore filters. The filters were washed twice with 3 ml of wash buffer containing 100 mM KCl, 10 mM HEPES (pH 7.3 with KOH), 5 mM $MgCl_2$, and 1 mM EGTA at room temperature. Radioactivity was measured in 5 ml Redi-Solv scintillation cocktail (Beckman, Fullerton, CA) with a Beckman LS-38 beta counter with 50% efficiency.

To study $^{45}Ca^{2+}$ uptake histochemically, frozen sections were allowed to thaw before being preincubated in permeabilization buffer containing 100 mM KCl, 10 mM HEPES, pH 7.3, 3% PEG, 1 mM DTT, and 10 μM digitonin for 10 min at 25°C. Sections were then transferred into uptake buffer containing 20 mM HEPES (pH 7.3 KOH), 75 mM K_2 oxalate, 3% PEG, 10 mM phosphocreatine, 10 U/ml creatine phosphokinase, 5 mM NaN_3, 0.2 mM total Ca^{2+}, 0.1 μCi/ml $^{45}Ca^{2+}$, 1 mM $MgCl_2$, 2 mM ATP, and 10 mM DTT at 37°C. Free Ca^{2+} concentration was adjusted to 0.3 μM with a Ca^{2+}-selective electrode. Incubations were performed in plastic slide mailing vessels (Evergreen, Los Angeles, CA) and buffer volumes were adjusted to give ~100 μg/ml protein in the assay. After incubation, slides were removed from uptake buffers and transferred into wash buffers containing 100 mM KCl, 10 mM K_2 oxalate, 3% PEG, 5 mM $MgCl_2$, 10 mM HEPES-KOH (pH 7.3), and 2 mM EGTA at 4°C. After washing in this buffer for 10 min, brain sections were wiped from the wet slides with absorbent tissue paper and radioactivity was measured in 15 ml Redi-Solv scintillation cocktail. Each experiment used to generate mean values utilized serially prepared tissue sections from different rat brains.

To image the distribution of accumulated $^{45}Ca^{2+}$, washed sections were dried under a cool air stream blown from one edge of the slide with careful, gentle vacuum aspiration of excess fluid from the other side and then were apposed to beta particle sensitive film (BetaMax; Amersham, Arlington Heights, IL) and developed in Kodak D-19 developer after 12–24-h exposure.

IP_3 and Ryanodine Autoradiography

IP_3 binding sites were visualized as described previously (Verma *et al.*, 1990a) with [^{3}H]Ins(1,4,5)P_3 (NEN-DuPont, Boston, MA). Ryanodine binding sites were visualized as described (Padua *et al.*, 1991) with minor modifications. Tissue sections were incubated for 2 h at 37°C in 1 M KCl, 20 mM MOPS-KOH (pH 7.5), 100 μM $CaCl_2$, 50 μM PMSF, 1 mM adenylyl-imidodiphosphate (APPNHP), and 15 nM [^{3}H]ryanodine (57 Ci/mmol; NEN-DuPont). Nonspecific binding was determined by including 50 μM unlabeled ryanodine (Calbiochem, Los Angeles, CA) in the reaction. Sections were washed in 50 mM KCl, 20 mM 3-(*N*-morpholino) propanesulfonic acid (MOPS)-KOH (pH 7.5), and 50 μM $CaCl_2$ at 4°C for 30 min, dried under a cool air stream, and exposed to tritium-sensitive film (Hyperfilm; Amersham, Arlington Heights, IL).

Unlabeled IP_3 was from LC Services (Woburn, MA), ryanodine was from Calbiochem (Los Angeles, CA). Radiolabeled items were from NEN-DuPont (Boston, MA); caffeine was from Aldrich (St. Louis, MO); local anesthetics, ruthenium red, and all other compounds were from Sigma (St. Louis, MO).

RESULTS

Regulation of Ca^{2+} Effects on $^{45}Ca^{2+}$ Accumulation into ER by Mg^{2+}, ATP, Local Anesthetics, and Ruthenium Red Reflects a CICR Process

We labeled ER stores of Ca^{2+} selectively in rat brain microsomes with the use of techniques similar to those described previously (Verma *et al.*, 1990a,b). We measured only ATP-dependent Ca^{2+} uptake, because under our conditions all Ca^{2+} accumulation is abolished by vanadate (5 mM) and lowered 90% by 10 nM thapsigargin, both of which are inhibitors of the ER Ca^{2+} pump. Ca^{2+} accumulation is unaffected by 10 mM sodium azide and 10 μg/ml oligomycin, inhibitors of mitochondrial but not ER Ca^{2+} pumps. Because the $^{45}Ca^{2+}$ accumulation is unaffected by 50 μM digitonin, it is unlikely to involve plasma membrane vesicle accumulation. To demonstrate CICR in rat brain microsomes, we employed a strategy similar to that of Wimsatt *et al.* (1990), who showed decreasing accumulation of Ca^{2+} by permeabilized rat heart myocytes at higher free Ca^{2+} concentrations. The CICR channel is presumably held open at the higher free Ca^{2+} levels resulting in less net $^{45}Ca^{2+}$ accumulation into the CICR pool because of leakage through the open CICR channel. This decrease

in free $^{45}Ca^{2+}$ accumulation at higher Ca^{2+} concentrations is blocked by local anesthetics and ruthenium red, which are known to block the CICR channel (Wimsatt *et al.*, 1990).

In rat brain microsomes $^{45}Ca^{2+}$ accumulation increases with rising free Ca^{2+} levels, peaking between 1 and 10 μM Ca^{2+} (Figure 1A). Half maximal $^{45}Ca^{2+}$ accumulation is apparent at ~0.6 μM Ca^{2+}. The K_m for $^{45}Ca^{2+}$ uptake in heart microsomes is similar to that of brain microsomes, but total Ca^{2+} accumulation is much greater in heart (Figure 1B). Heart microsomes also differ from brain in displaying a broader plateau of Ca^{2+} uptake over the free Ca^{2+} range of 1–30 μM Ca^{2+}. Between 10 and 100 μM free Ca^{2+}, $^{45}Ca^{2+}$ accumulation decreases in both brain and heart microsomes, whereas Ca^{2+} adenosine triphosphatase (ATPase) activity is unchanged (Figure 1, insets; Wimsatt *et al.*, 1990). Adenine nucleotides stimulate CICR, (Fill and Coronado, 1988) and 10 mM ATP prevents the increase in $^{45}Ca^{2+}$ accumulation between 1 and 10 μM free Ca^{2+}. Magnesium (5 mM), an inhibitor of CICR, prevents the decreased $^{45}Ca^{2+}$ accumulation at higher free Ca^{2+}. Thus Ca^{2+} accumulation in brain progressively increases to levels three times those seen with 1 mM Mg^{2+} at 100 μM free Ca^{2+} (Figure 1A). Enhancement of net Ca^{2+} accumulation by 5 mM magnesium in heart microsomes is apparent at lower free calcium levels than in brain (Figure 1B). These effects of magnesium are seen only at higher free Ca^{2+} levels and require magnesium concentrations greatly in excess of those required for maximal Ca^{2+} ATPase activity (Figure 1, inset) but similar to those required to inhibit CICR (Smith *et al.*, 1986; Moutin and Dupont, 1988).

At 30 μM free Ca^{2+} the optimal Mg^{2+} concentration for preventing CICR is 5–10 mM in heart and 5 mM in rat brain (Figure 2, A and B). The greater efficacy of Mg^{2+} in enhancing $^{45}Ca^{2+}$ accumulation in heart than brain suggests differences in the CICR process in these two tissues. Thus Mg^{2+}-sensitive CICR occurs to a greater extent and at lower free Ca^{2+} concentrations in heart as compared with brain microsomes. Other CICR inhibitors resemble Mg^{2+} in their actions on $^{45}Ca^{2+}$ uptake. Thus at 30 μM free Ca^{2+}, 200 μM ruthenium red enhances $^{45}Ca^{2+}$ accumulation by 50% in heart and brain microsomes (Figure 2, A and B). Similarly, the local anesthetics tetracaine and procaine block CICR with optimal concentrations of 200–300 μM and 1–10 mM, respectively. Unlike Mg^{2+} these local anesthetics are more efficacious in brain than in heart also suggesting pharmacological heterogeneity of the CICR process among these tissues.

IP_3-Sensitive Ca^{2+} Mobilization and CICR are Active over Different Ca^{2+} Concentrations

To estimate the proportion of Ca^{2+} accumulation associated with the CICR pool, we subtracted $^{45}Ca^{2+}$ levels in the presence of 1 mM Mg^{2+} from those seen with 5 mM Mg^{2+} in brain microsomes (Figure 3, A and C). The apparent CICR pool of Ca^{2+} increases progressively be-

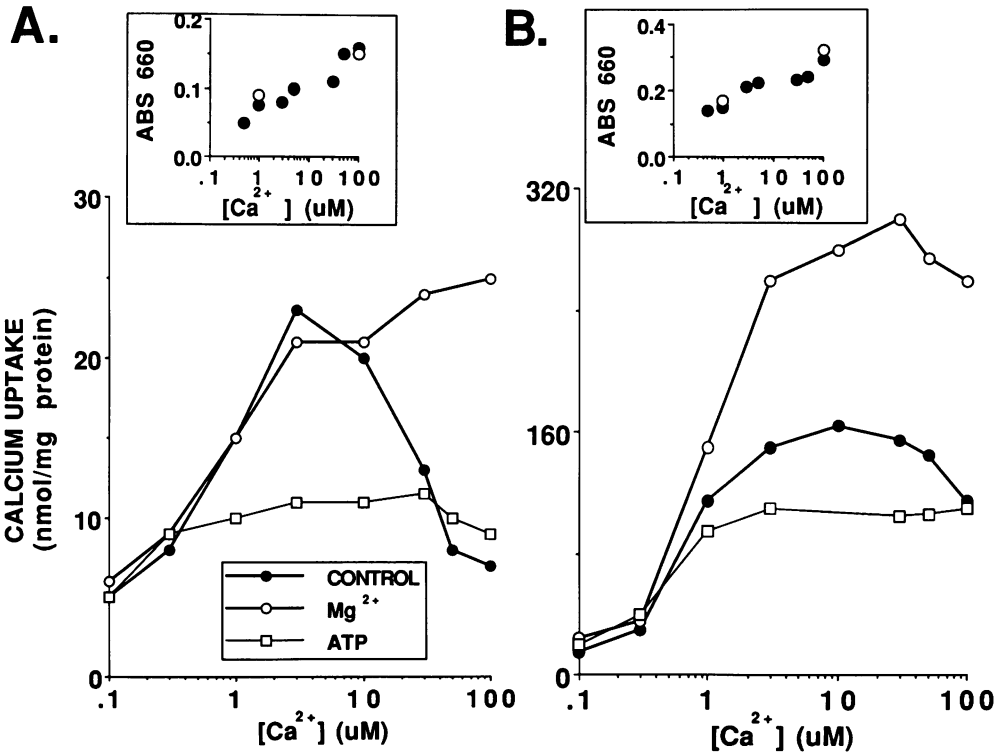

Figure 1. Modulation of $^{45}Ca^{2+}$ uptake in rat brain and heart microsomes by calcium, ATP and magnesium. Ca^{2+} transport and Ca^{2+} ATPase assays were performed as described in METHODS at different free Ca^{2+} concentrations. Assays were performed under control conditions (2 mM Mg ATP) or with adjustment of ATP to 10 mM or Mg^{2+} to 5 mM. (A) Rat brain microsomes (B) Rat heart microsomes. Insets: Ca^{2+}-ATPase activity. (●, 2 mM Mg^{2+}; ○, 5 mM Mg^{2+}). Results shown are typical of four experiments performed in duplicate with variability of <5%.

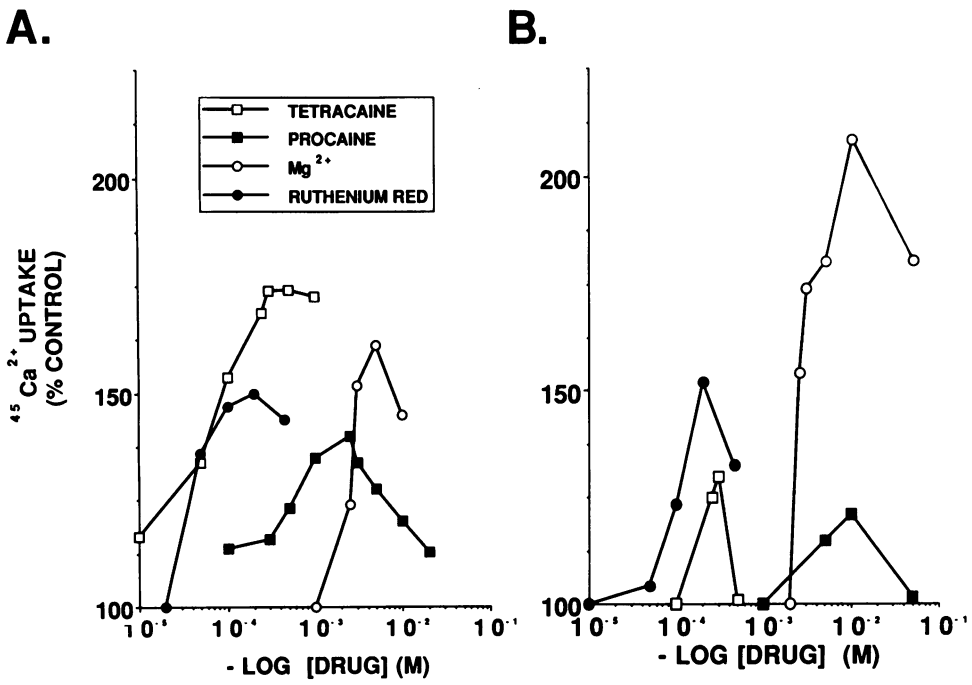

Figure 2. Modulation of $^{45}Ca^{2+}$ uptake by CICR inhibitors. $^{45}Ca^{2+}$ uptake was performed in rat brain and heart microsomes as described at 30 μM free Ca^{2+}. Ruthenium red, procaine, tetracaine, and magnesium were added at indicated concentrations. (A) Rat brain microsomes (B) Rat heart microsomes. Data shown are representative of 3–5 experiments performed in duplicate with variability of <5%.

tween 10–100 μM free Ca^{2+} with half maximal increase at 20 μM. At high concentrations, caffeine activates CICR (Johnson and Inesi, 1969; Fabiato, 1983; Smith *et al.*, 1986; Wimsatt *et al.*, 1990). When 50 mM caffeine is present during $^{45}Ca^{2+}$ uptake, it reduces net Ca^{2+} accumulation over the free Ca^{2+} range of 0.3–30 μM (Figure 3, A and B). Beyond this range CICR is already activated by the existing free Ca^{2+} levels. Caffeine al-

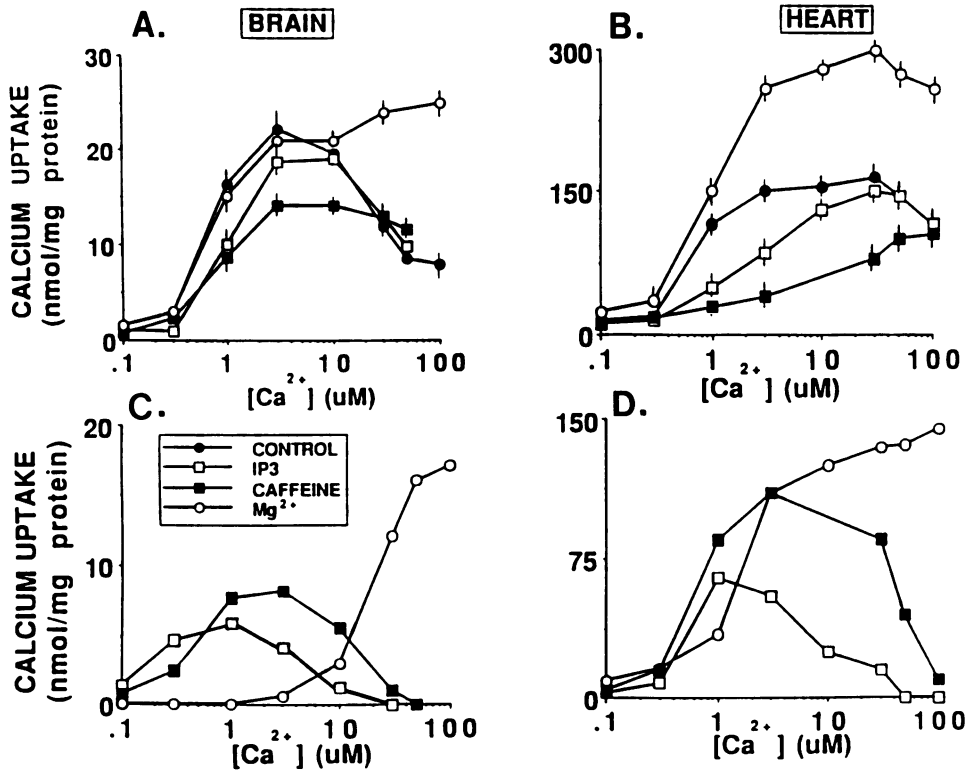

Figure 3. Calcium sensitivity of CICR and IP_3-regulated Ca^{2+} pools. Ca^{2+} uptake was carried out with the use of rat brain and heart microsomes at varying free Ca^{2+} concentrations. Assays were performed under control conditions (2 mM Mg ATP) or with 5 mM Mg^{2+}, 10 μM IP_3, or 50 mM caffeine. The difference between control and experimental conditions in rat brain microsomes (A) and rat heart microsomes (B) is plotted in (C) and (D), respectively. Data shown are representative of four experiments performed in duplicate with variability of <10%.

losterically enhances conductance of CICR channels by increasing their affinity for Ca^{2+} (Pessah *et al.*, 1987; Seino *et al.*, 1991). Caffeine (50 mM) allows CICR to take place at lower free Ca^{2+} levels in both heart and brain microsomes (Figure 3, A and B).

To evaluate the size of the IP_3-sensitive pool of Ca^{2+} at varying Ca^{2+} levels, we monitored $^{45}Ca^{2+}$ accumulation in the absence and presence of 10 μM IP_3, a concentration that maximally releases Ca^{2+} from rat brain microsomes (Figure 3, A and C) (Verma *et al.*, 1990b). IP_3 markedly decreases $^{45}Ca^{2+}$ accumulation in brain microsomes between 0.1 and 10 μM free Ca^{2+} with minimal effects apparent at higher Ca^{2+} concentrations (Figure 3, A and C). Heart microsomes also show sensitivity to IP_3 (Figure 3, B and D) in addition to their large caffeine-sensitive and Mg^{2+}-inhibitable CICR calcium stores (Figure 3, B and D). However, the effects of IP_3 and caffeine are optimal over different free Ca^{2+} ranges.

Rat Brain IP_3-Sensitive and CICR Pools are Regionally Segregated

We examined $^{45}Ca^{2+}$ uptake in microsomes from different brain regions over varying free Ca^{2+} concentrations in the absence and presence of 10 μM IP_3 or 0.5 mM tetracaine (Figure 4). As in whole brain microsomes, preparations from olfactory bulb and hippocampus display reduced $^{45}Ca^{2+}$ accumulation at concentrations exceeding 10 μM free Ca^{2+}, an effect blocked by tetracaine (0.5 mM). This decrease is not apparent in cerebellar microsomes, but the enhancing effect of tetracaine on net Ca^{2+} accumulation suggests that some CICR does occur in cerebellum. IP_3 (10 μM) markedly diminishes net $^{45}Ca^{2+}$ sequestration in cerebellar microsomes with lesser effects in hippocampus and negligible influence in olfactory bulb. Thus prominent CICR and negligible IP_3-sensitive Ca^{2+} pools are present in olfactory bulb. Hippocampal microsomes display both release mechanisms, whereas the IP_3-sensitive pool accounts for the majority of the cerebellar releasable Ca^{2+}. Interestingly, in hippocampus, participation of Ca^{2+} in the presumed CICR pool commences with Ca^{2+} levels at which participation in the IP_3-sensitive pool declines (Figure 4).

Table 1. Pharmacology of $^{45}Ca^{2+}$ accumulation in rat brain microsomes and sections

	% Control	
	Microsomes	Sections
IP_3 (10 μM)	68	70
Caffeine (50 mM)	62	60
IP_3 + heparin (100 μg/ml)	100	100
Caffeine + heparin	62	60
IP_3 + caffeine	35	34

$^{45}Ca^{2+}$ uptake was performed in brain microsomes or sections as described in METHODS with the indicated additions with the use of oxalate buffers at 0.3 μM free Ca^{2+}. Microsomes were incubated for 15 min, and sections were incubated for 60 min. Results are typical of three experiments performed in triplicate.

Autoradiographic Localizations Differentiate CICR and IP_3-Sensitive ER Ca^{2+} Pools

To compare the histological distribution of CICR and IP_3-sensitive pools, we monitored oxalate supported

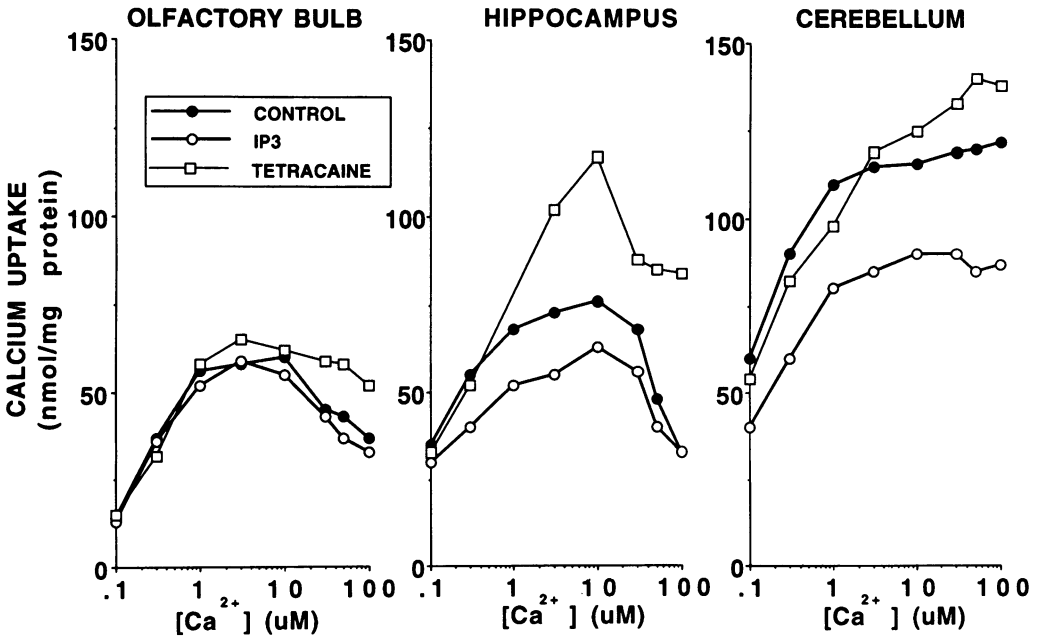

Figure 4. IP_3-sensitive and CICR Ca^{2+} pools in different brain regions. $^{45}Ca^{2+}$ uptake was assayed in regional brain microsomes over varying free Ca^{2+} concentrations in the absence and presence of 10 μM IP_3 or 0.5 mM tetracaine in olfactory, hippocampal, and cerebellar microsomes. Results are representative of three experiments performed in triplicate with a variability of <5%.

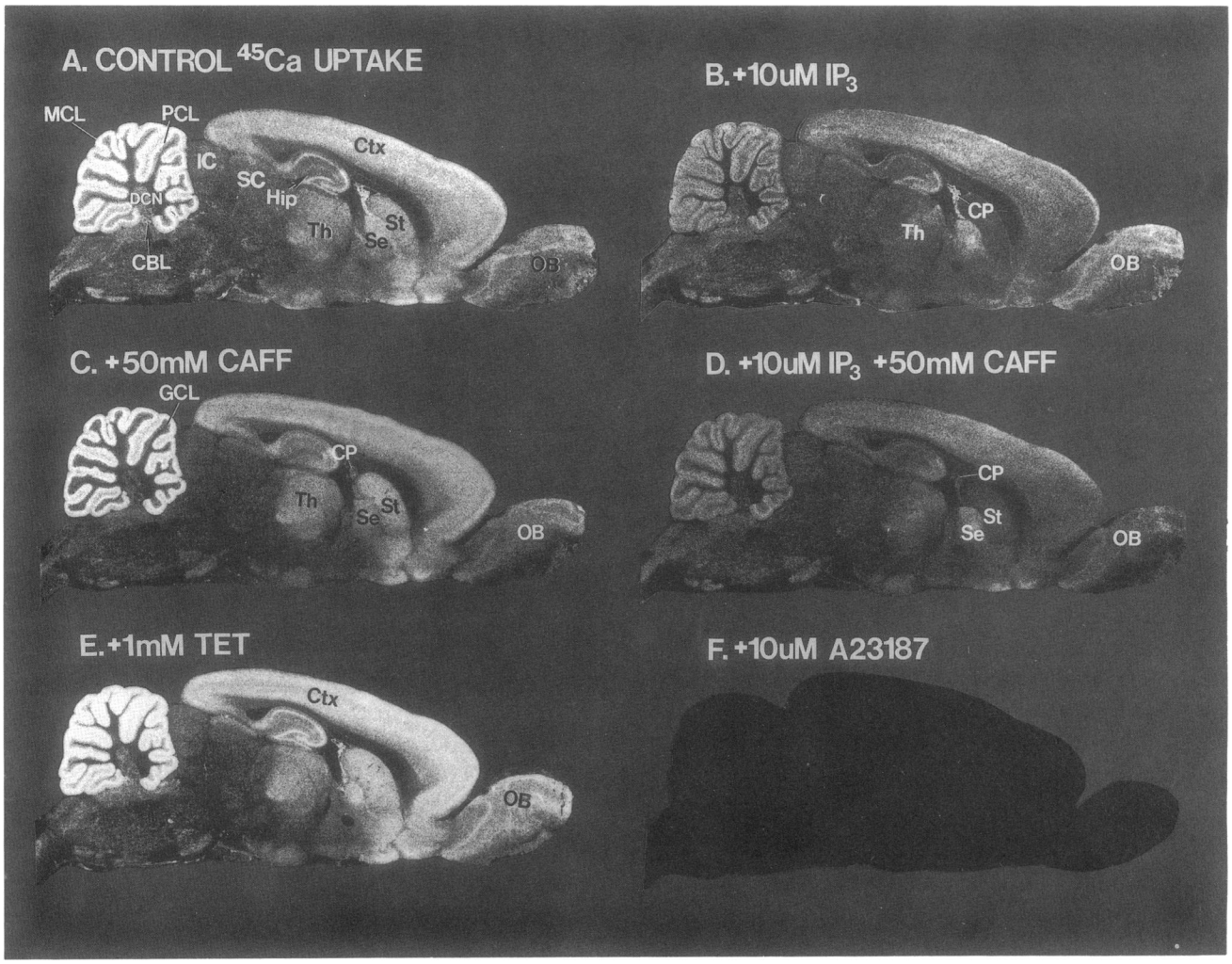

Figure 5. Autoradiographic localization of $^{45}Ca^{2+}$ accumulation by rat brain sections. Oxalate supported $^{45}Ca^{2+}$ uptake was monitored in midsagittal rat brain sections and visualized as described in METHODS (A) control, (B) +10 μM IP_3, (C) +50 mM caffeine, (D) +10 μM IP_3 and 50 mM caffeine, (E) +1 mM tetracaine, (F) +10 μM A23187. Abbreviations: Ctx, cerebral cortex; Cbl, cerebellum; Hip, hippocampus; OB, olfactory bulb; St, striatum; Se, septum; Th, thalamus; PCL, Purkinje cell layer; GCL, granule cell layer; MCL, molecular cell layer; CP, choroid plexus; IC, Inferior Colliculus; SC, Superior Colliculus; DCN, Deep cerebellar Nuclei; P, Pyramidal cell bodies; F, Fimbria.

$^{45}Ca^{2+}$ uptake into fresh frozen tissue sections, as previously described (Verma *et al.*, 1990b). To evaluate the relative prominence of these pools at near physiological Ca^{2+} levels we examined $^{45}Ca^{2+}$ accumulation at 0.3 μM free Ca^{2+}. Under these conditions $^{45}Ca^{2+}$ uptake into tissue sections, monitored by counting accumulated $^{45}Ca^{2+}$ in tissue wiped from slides, is comparable with that in microsomes. Oxalate buffers reveal effects of CICR modulators at lower free Ca^{2+} concentrations than the phosphate buffers. With oxalate buffers at 0.3 μM free Ca^{2+}, IP_3 (10 μM) produces 32 and 30% net reduction of $^{45}Ca^{2+}$ accumulation in brain microsomes and sections, respectively. Caffeine (50 mM) reduces net $^{45}Ca^{2+}$ uptake by 38 and 40% in brain microsomes and sections, respectively. IP_3 and caffeine are additive in their effects on $^{45}Ca^{2+}$ accumulation, whereas heparin (100 μg/ml), a specific inhibitor of IP_3 binding (Worley *et al.*, 1987) and IP_3 mediated Ca^{2+} release (Ghosh *et al.*, 1988), reverses the effects of IP_3 but not those of caffeine (Table 1).

Autoradiographic visualization of $^{45}Ca^{2+}$ accumulated by rat brain sections reveals anatomical heterogeneity in the amount of ER $^{45}Ca^{2+}$ uptake, as previously reported (Figure 5A) (Verma *et al.*, 1990b). Highest uptake is apparent in the Purkinje cell layer of the cerebellum, with enrichment also evident in the cerebral cortex, hippocampus, septum, striatum, and olfactory bulb. By contrast, the brainstem and hypothalamus have notably low levels of $^{45}Ca^{2+}$. Also as previously observed, IP_3 (10 μM) reduces $^{45}Ca^{2+}$ accumulation (Figure 5B) with effects most marked in the cerebellum, cerebral cortex, corpus striatum, hippocampus, and anterior basal fore-

brain. Caffeine-sensitive $^{45}Ca^{2+}$ pools display a different regional distribution than the IP_3-sensitive pools (Figure 5C). Thus the granule cell layer of the cerebellum is predominantly sensitive to caffeine, as is the olfactory bulb, the dentate gyrus of the hippocampal process, and the septum. The cerebral cortex and other hippocampal layers appear sensitive to both IP_3 and caffeine, whereas some areas appear resistant to both of these agents (Figure 5D). Tetracaine (1 mM) enhances $^{45}Ca^{2+}$ uptake in several regions, most notably in the hippocampus, olfactory bulb, cerebral cortex, and septum (Figure 5E). The regions most affected by tetracaine resemble those most sensitive to caffeine. The calcium ionophore A23187 abolishes all $^{45}Ca^{2+}$ accumulation demonstrating that all of the $^{45}Ca^{2+}$ associated with the sections is sequestered into a vesicular pool (Figure 5F).

Rat brain sections display specific binding sites for both [^{3}H]IP_3 (5 pmol/mg protein) and [^{3}H]ryanodine (105 fmol/mg protein) (Figure 6, C and F). The effects of IP_3 on $^{45}Ca^{2+}$ flux are localized to regions enriched in [^{3}H]IP_3 binding (Figure 6, A–C), whereas, the effects of caffeine and tetracaine colocalize with [^{3}H]ryanodine binding sites (Figure 6, D–F). IP_3 receptor sites and IP_3-sensitive calcium pools are both enriched in the CA-1 region of the hippocampus with lower levels in CA-3, CA-4, and the dentate gyrus. Ryanodine binding sites and caffeine- and tetracaine-sensitive $^{45}Ca^{2+}$ flux are enriched in the dentate gyrus, CA-3, and CA-4 regions. While the striatum shows an enrichment of IP_3 receptors and IP_3-sensitive Ca^{2+} pools over the septum, ryanodine receptors and CICR pools appear somewhat more enriched in the septum as compared with the striatum. Ryanodine binding sites are enriched in the choroid plexus where Ca^{2+} pools are more sensitive to caffeine and tetracaine than IP_3 (Figure 6, A–F).

Muscular Tissues Segregate Calcium Pools

Several striated muscle structures are rich in [^{3}H]ryanodine sites, as seen in a sagittal section through a neonatal rat (Figure 7A). The lingual, intercostal, diaphragmatic, and axial musculature display [^{3}H]ryanodine receptor densities comparable with heart muscle. Binding in neonatal brain is much lower with an apparent absence of sites in the olfactory bulb or cerebellum at postnatal day 1. [^{3}H]IP_3 binding sites are barely detectable in the neonatal rat with high levels of nonspecific binding (data not shown).

Rat heart sections display specific binding sites for both [^{3}H]IP_3 and [^{3}H]ryanodine. CICR channels labeled

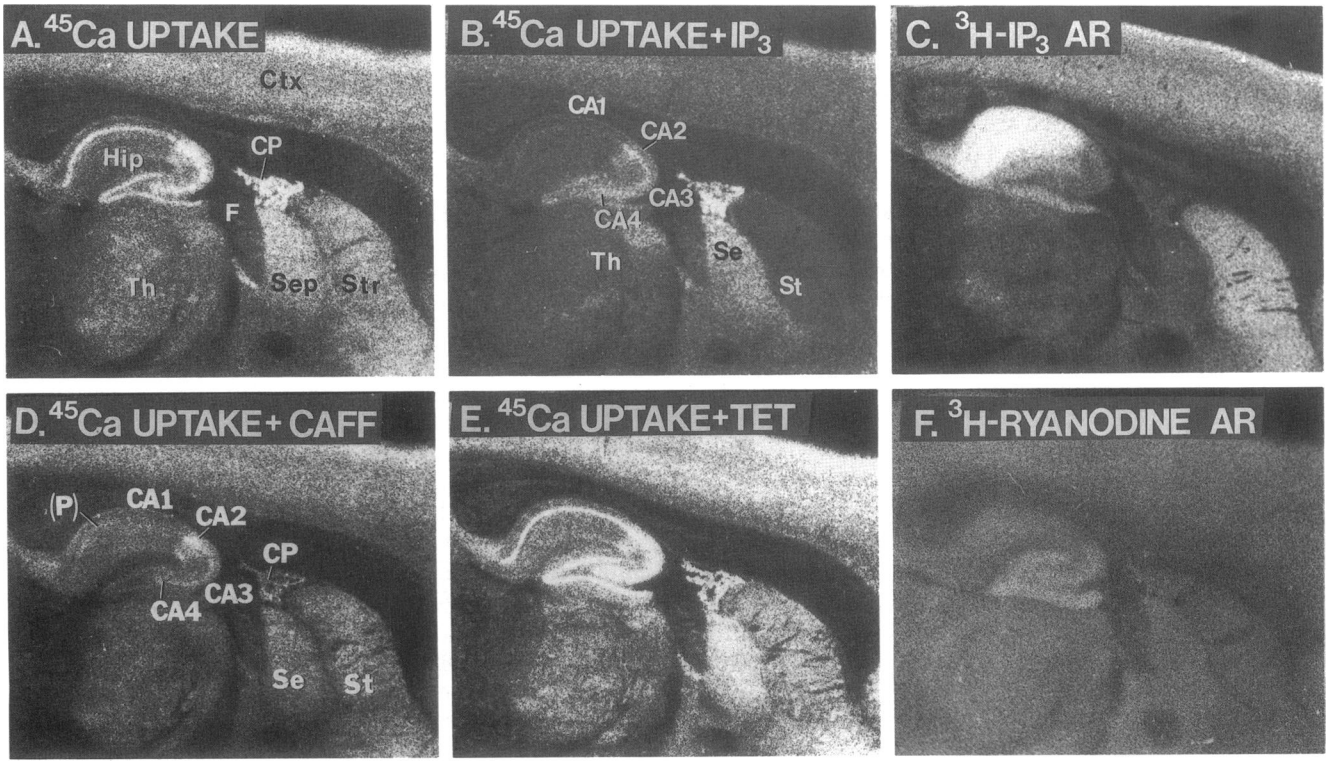

Figure 6. Localization of CICR and IP_3-sensitive Ca^{2+} pools in rat brain. $^{45}Ca^{2+}$ uptake was measured in midsagittal rat brain sections in the absence (A) and presence of 10 μM IP_3 (B), 50 mM caffeine (D), or 1 mM tetracaine (E). [^{3}H]IP_3 autoradiography (C) and [^{3}H]ryanodine autoradiography (F) were performed as described. Blanks for ligand autoradiography assessed with 10 μM unlabeled IP_3 or ryanodine did not differ from film background (not shown). Abbreviations are the same as in Figure 5.

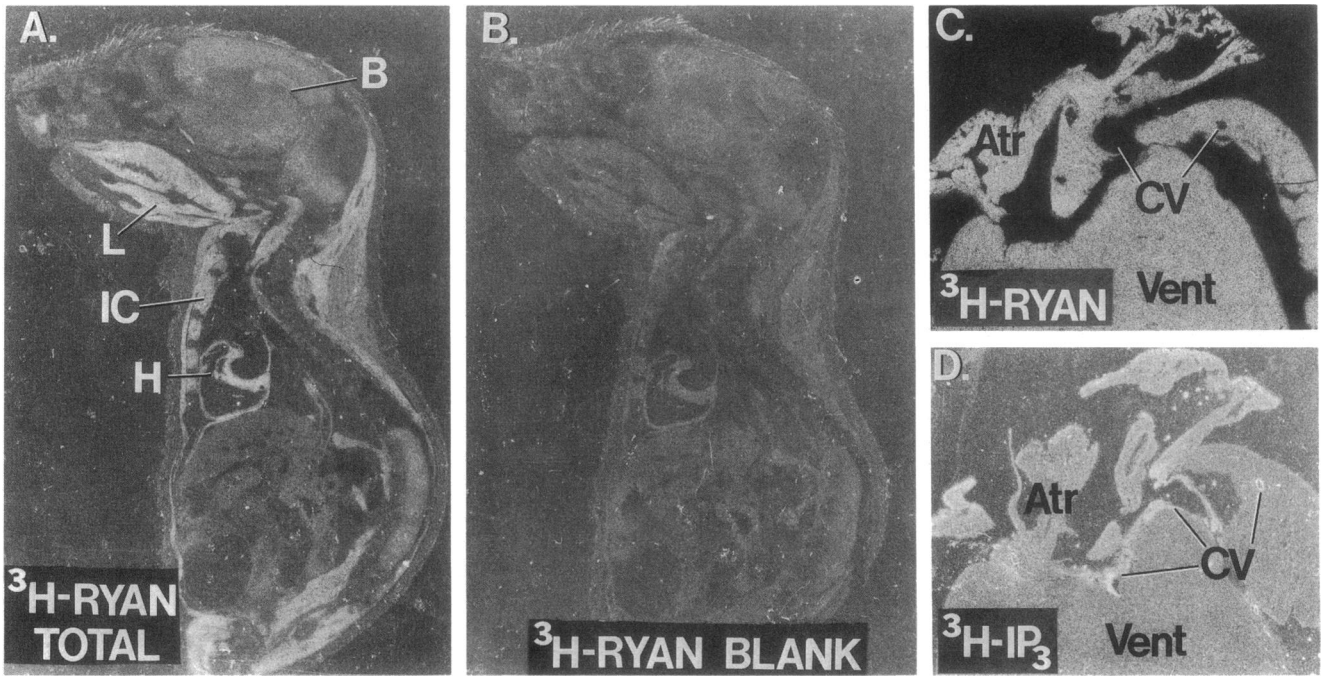

Figure 7. Localization of [^{3}H]ryanodine and [^{3}H]IP$_3$ receptors in rat muscular structures. Autoradiography of [^{3}H]ryanodine and [^{3}H]IP$_3$ binding sites was performed as described. (A) [^{3}H]Ryanodine binding sites in neonatal rat (postnatal day 1) whole-body sagittal sections. (B) [^{3}H]Ryanodine binding in the presence of 10 μM cold ligand. (C) [^{3}H]Ryanodine binding sites in rat heart sections. (D) [^{3}H]IP$_3$ binding sites in rat heart sections. Blanks for (C) and (D) performed with 10 μM ryanodine and 10 μM IP$_3$, respectively, were not different from film background. Abbreviations: L, lingual; IC, intercostal; B, brain; H, heart; Atr, atria; CV, coronary vessels; Vent, ventricles.

by [^{3}H]ryanodine are highly enriched in atrial and ventricular cardiac muscle but are absent from the smooth muscle of the coronary arteries (Figure 7C). IP$_3$-sensitive Ca^{2+} channels, shown by [^{3}H]IP$_3$ autoradiography, are less abundant in cardiac muscle but show a selective enrichment in the vascular smooth muscle (Figure 8D). This segregation of IP$_3$ and ryanodine receptors is particularly striking in chicken heart sections with their more prominent coronary vascular and conduction fiber tissue enriched in [^{3}H]IP$_3$ binding while lacking [^{3}H]ryanodine receptors (Figure 8 A–D). Conversely, chicken cardiac muscle is selectively enriched in [^{3}H]ryanodine sites over [^{3}H]IP$_3$ sites.

DISCUSSION

This study demonstrates CICR pools of Ca^{2+} in the brain with localizations that contrast with IP$_3$-sensitive pools. Our biochemical experiments provide several lines of evidence for a CICR pool of Ca^{2+}. The decreased net accumulation of $^{45}Ca^{2+}$ into microsomes with increasing concentrations of Ca^{2+} is consistent with CICR competing with Ca^{2+} accumulation by the pump at the higher Ca^{2+} concentration. Support for this notion comes from the ability of Mg^{2+} to prevent the decrease in $^{45}Ca^{2+}$ accumulation. Mg^{2+} blocks the CICR process in cardiac microsomes and isolated calcium channels (Smith *et al.*, 1986; Moutin and Dupont, 1988). Similarly ruthenium red, procaine, and tetracaine inhibit the decreased $^{45}Ca^{2+}$ accumulation at high Ca^{2+} concentrations. Ruthenium red, tetracaine, and other local anesthetics have also been demonstrated to block the CICR process in skeletal and cardiac muscle, intact myocytes, microsomes, and isolated channels with potencies similar to those seen in our experiments (Johnson and Inesi, 1969; Wimsatt *et al.*, 1990). Importantly, brain and heart microsomal CICR processes are distinguished by their relative sensitivity to various CICR inhibitors. Thus, while ruthenium red affects brain and heart CICR similarly, the brain CICR is more sensitive to local anesthetics and the heart CICR more sensitive to magnesium. Caffeine and ATP prevent $^{45}Ca^{2+}$ accumulation at a wide range of Ca^{2+} concentrations consistent with a facilitation of the CICR process. This fits with demonstrations that caffeine and ATP allosterically enhance CICR channels by increasing their affinity for Ca^{2+} (Kim *et al.*, 1983; Pessah *et al.*, 1987; Seino *et al.*, 1991). Our experiments in the physiological phosphate buffers utilizing tetracaine and Mg^{2+} suggest that the CICR process is first apparent at concentrations of $Ca^{2+} > 1$ μM. The ability of caffeine and ATP to diminish Ca^{2+} accumulation at concentrations as low as 0.1 μM Ca^{2+} suggests that these agonists may enhance the affinity of Ca^{2+} for CICR sites. The virtually identical regional localizations

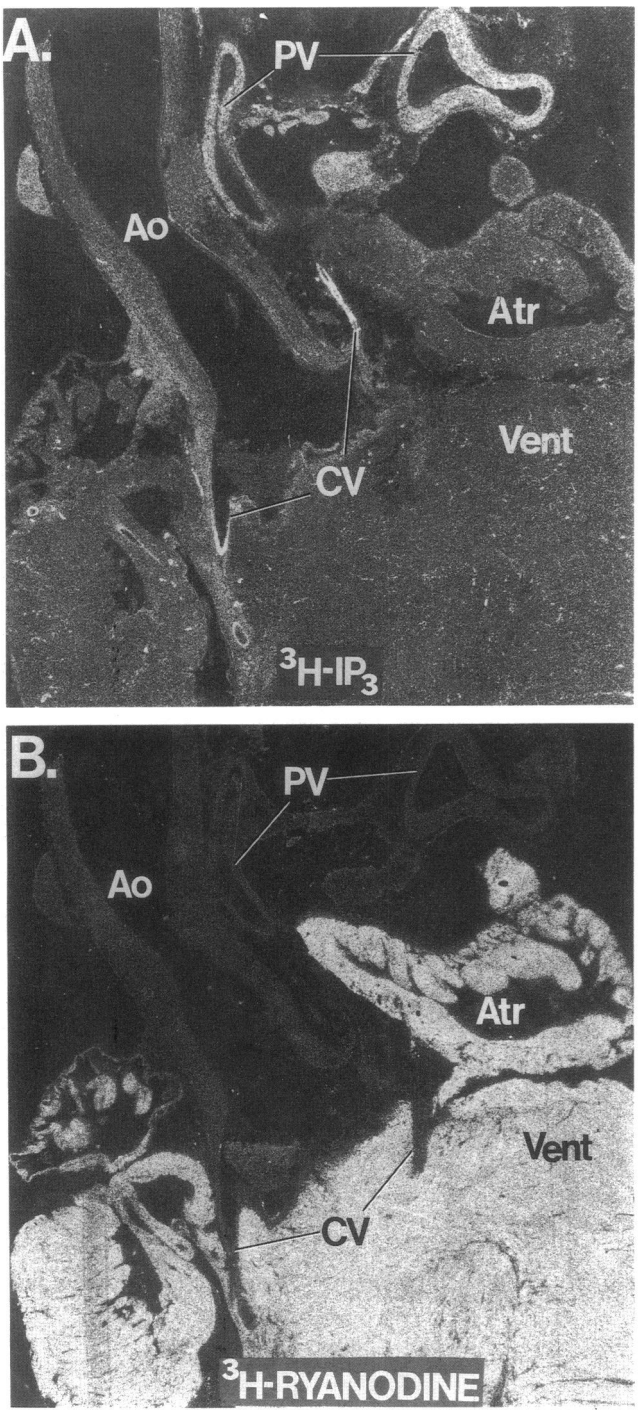

Figure 8. Localization of [^{3}H]ryanodine and [^{3}H]IP_3 receptors in chicken heart. (A) [^{3}H]IP_3 binding to chicken heart sections; (B) [^{3}H]Ryanodine binding to chicken heart sections. Blanks performed with 10 μM IP_3 or 10 μM ryanodine were not different from film background. Abbreviations: Atr, atria; Ao, aorta; CV, coronary vessels; PV, pulmonary vessels; Vent, ventricle.

of the putative CICR pool of Ca^{2+} (caffeine releasable, tetracaine, and Mg^{2+} stimulated) and [^{3}H]ryanodine binding sites strongly support the conclusion that caffeine releasable $^{45}Ca^{2+}$ labels the CICR pool under our experimental conditions.

The various pharmacological agents employed here have diverse actions. Tetracaine and procaine influence several membrane functions including Ca^{2+} ATPase activity. The action of these agents as CICR inhibitors is manifested at substantially lower concentrations than their effects on other processes (Lavoie *et al.*, 1986). Thus these agents enhance net Ca^{2+} accumulation in rat brain microsomes and lysed synaptosomes at low concentrations e.g., 10 μM tetracaine, but inhibit Ca^{2+}-ATPase only at millimolar levels (Figure 2; Lavoie *et al.*, 1986). The concentration ranges of tetracaine and procaine for enhancing net $^{45}Ca^{2+}$ uptake in our experiments closely resemble protencies observed by others for inhibiting CICR (Johnson and Inesi, 1969; Chamberlain *et al.*, 1984; Altschuld *et al.*, 1985; Wimsatt *et al.*, 1990). Caffeine blocks adenosine receptors and inhibits phosphodiesterases in addition to activating CICR. The concentrations of caffeine employed in our study are the same as those required to modulate CICR in other systems (Johnson and Inesi, 1969; Mekhail-Ishak *et al.*, 1987; Pessah *et al.*, 1987).

The effects of IP_3 are optimal over lower free Ca^{2+} concentrations than the CICR process. Presumably, as IP_3 releases Ca^{2+} to concentrations exceeding 0.5 μM inside live cells, the released Ca^{2+} would inhibit further actions of IP_3. This fits with earlier observations that Ca^{2+} inhibits [^{3}H]IP_3 binding to its receptors in brain with an IC_{50} of 300 nM (Worley *et al.*, 1987). The CICR process becomes most prominent at Ca^{2+} concentrations wherein IP_3 effects decline, suggesting that Ca^{2+} released by IP_3 both turns off the IP_3 release process and initiates the CICR process. This would provide a "feed forward," positively cooperative enhancement of Ca^{2+} release. Such a model fits with speculations of several workers that interactions between IP_3-induced Ca^{2+} release and CICR account for intracellular Ca^{2+} oscillations (Berridge and Galione, 1988; Goldbeter *et al.*, 1990; Randriamampita *et al.*, 1991). Such Ca^{2+} oscillations might be influenced by the relative enrichment of either type of Ca^{2+} pool in a given tissue.

One of our most striking findings involves differential and frequently reciprocal localizations of IP_3-sensitive Ca^{2+} pools and CICR pools. For instance, CA-1 of the hippocampus is enriched in the IP_3 pool whereas CA-3 and dentate gyrus have higher densities of CICR. Similarly, the corpus striatum is enriched in the IP_3-sensitive Ca^{2+} pool whereas the closely adjacent medial septum has higher densities of CICR. Cerebellum and olfactory bulb are selectively enriched in IP_3 and CICR pools, respectively. In avian cerebellar Purkinje cells, Walton *et al.* (1991) observed ryanodine receptors in the same cells as IP_3 receptors. The much greater density

of ryanodine receptors in chick than in mammalian brain suggests species differences. Because Walton *et al.* (1991) did not examine multiple brain regions, it is unclear whether chick, like rat, displays reciprocal densities of the two receptors in diverse areas.

Cardiac tissue from both rat and chicken possesses prominent CICR associated mainly with the striated ventricular and atrial muscle. Striated muscle tissues in general are enriched in CICR, which is evident in neonatal rats. By contrast, IP_3 pools in cardiac tissue are enriched in the smooth muscle of coronary vasculature and cardiac conduction fibers with much lower levels in striated muscle. It should be emphasized that areas with apparently low densities of one of the pools of Ca^{2+} would not be anticipated to be devoid of these pools but merely to have lower amounts of them. Insofar as given brain regions differ in the prominence of one of the two pools of Ca^{2+}, the interaction between those two pools in mediating physiological Ca^{2+} release and Ca^{2+} oscillations (Berridge and Galione, 1988) may differ in various brain regions.

ACKNOWLEDGMENTS

Supported by USPHS grants DA-00266 and MH-18501, Research Scientist Award DA-00074 to S.H.S., Training Grant GS-07141 to A.V., a grant from the International Life Sciences Institute, and a gift from Bristol-Myers-Squibb.

REFERENCES

Altschald, R.A., Wenger, W.C., Lamka, K.G., Kindig, O.R., Capen, C.C., Mizuhira, V., Vander Heide, R.S., and Brierly, G.P. (1985). Structural and functional properties of adult rat heart myocytes lysed with digitonin. J. Biol. Chem. *260*, 14325–14334.

Ashley, R.H. (1989). Activation and conductance properties of ryanodine sensitive-calcium channels from brain microsomal membranes incorporated into planar lipid bilayers. J. Membr. Biol. *111*, 179–189.

Berridge, M.J., and Galione, A. (1988). Cytosolic calcium oscillators. FASEB J. *2*, 3074–3082.

Berridge, M.J., and Irvine, R.F. (1989). Inositol phosphates and cell signalling. Nature *341*, 197–205.

Chamberlain, B.K., Volpe, P., and Fleischer, G. (1984). Inhibition of calcium-induced calcium release from purified cardiac sarcoplasmic reticulum. J. Biol. Chem. *259*, 7547–7553.

Chu, A., Diaz-Munoz, M., Hawkes, M.J., Brush, K., and Hamilton, S.L. (1990). Ryanodine as a probe for the functional state of the skeletal muscle sarcoplasmic reticulum calcium release channel. Mol. Pharmacol. *37*, 735–741.

Ellisman, M.E., Deerinck, T.J., Ouyang, Y., Beck, C.F., Tanksley, S.J., Walton, P.D., Airey, J.A., and Sutko, J.Z. (1990). Identification and localization of ryanodine binding proteins in the avian nervous system. Neuron *5*, 135–146.

Endo, M. (1977). Release of calcium from the sarcoplasmic reticulum. Physiol. Rev. *57*, 71–108.

Fabiato, A. (1983). Calcium-induced release of calcium from the cardiac sarcoplasmic reticulum. Am. J. Physiol. *245*, C1–C14.

Fill, M., and Coronado, R. (1988). Ryanodine receptor channel of sarcoplasmic reticulum. Trends Neurosci. *11*, 453–457.

Ghosh, T.K., Eis, P.S., Mullaney, J.M., Ebert, C.L., and Gill, D.L. (1988). Competitive, reversible and potent antagonism of inositol 1,4,5-triphosphate activated calcium release by heparin. J. Biol. Chem. *263*, 11075–11079.

Goldbeter, A., Dupont, G., and Berridge, M.J. (1990). Minimal model for signal-induced Ca^{2+} oscillations and for their frequency in coding through protein phosphorylation. Proc. Natl. Acad. Sci. USA *87*, 1461–1465.

Holliday, J., Adams, R.J., Sejnowski, T.J., and Spitzer, N.C. (1991). Calcium-induced release of calcium regulates differentiation of cultured spinal neurons. Neuron *7*, 787–796.

Inui, M., Saito, A., and Fleisher, S. (1987). Purification of the ryanodine receptor and identity with feet structures of junctional terminal cisternae of sarcoplasmic reticulum from fast skeletal muscle. J. Biol. Chem. *262*, 1740–1747.

Johnson, P.N., and Inesi, G. (1969). The effect of methylxanthines and local anesthetics on fragmented sarcoplasmic reticulum. J. Pharmacol. Exp. Ther. *169*, 308–314.

Kim, D.H., Ohnishi, S.T., and Ikemoto, N. (1983). Kinetic studies of calcium release from sarcoplasmic reticulum in vitro. J. Biol. Chem. *258*, 9662–9668.

Kinya, O., Huntington, F., Khanna, V.K., Zorzato, F., Green, N.M., and MacLennan, D.H. (1990). Molecular cloning of cDNA encoding the Ca^{2+} release channel (ryanodine receptor) of rabbit cardiac muscle sarcoplasmic reticulum. J. Biol. Chem. *265*, 13572–13483.

Lai, F.A., Xu, L., and Meissner, G. (1990). Identification of a ryanodine receptor in rat and bovine brain. Biophys. J. *57*, 529a.

Lavoie, P.A., Mekhail-Ishak, K., and Sharkawi, M. (1986). Biphasic effects of local anesthetics on the adenosine triphosphate-dependent calcium uptake by lysed brain synaptosomes. Can. J. Physiol. Pharmacol. *64*, 218–221.

McPherson, P.S., and Campbell, K.P. (1990). Solubilization and biochemical characterization of the high affinity [^{3}H]ryanodine receptor protein from rabbit brain membranes. J. Biol. Chem. *265*, 18454–18460.

McPherson, P.S., Kim, Y., Valdivia, H., Knudson, C.M., Takekura, H., Franzihi-Armstrong, C., Coronado, R., and Campbell, K.P. (1991). The brain ryanodine receptor: a caffeine-sensitive calcium release channel. Neuron *7*, 17–25.

Mekhail-Ishak, K., Lavoie, P.A., and Sharkawi, M. (1987). Effects of caffeine and cyclic adenosine 3',5'-monophosphate on adenosine triphosphate-dependent calcium uptake by lysed brain synaptosomes. Brain Res. *426*, 62–68.

Meldolesi, J., Madeddu, L., and Pozzan, T. (1990). Intracellular Ca^{2+} storage organelles in non-muscle cells: heterogeneity and functional assignment. Biochem. Biophys. Acta. *1055*, 130–140.

Moutin, M.J., and Dupont, Y. (1988). Rapid filtration studies of Ca^{2+} induced Ca^{2+} release from skeletal sarcoplasmic reticulum. J. Biol. Chem. *263*, 4228–4235.

Padua, R.A., Wan, W., Nagy, T.I., and Geiger, J.D. (1991). [^{3}H]Ryanodine binding sites in rat brain demonstrated by membrane binding and autoradiography. Brain Res. *542*, 135–140.

Pessah, I.N., Stambuk, R.A., and Casdia, J.E. (1987). Ca^{2+}-activated ryanodine binding: mechanisms of sensitivity and intensity modulation by Mg^{2+}, caffeine and adenine nucleotides. Mol. Pharmacol. *31*, 232–238.

Randriamampita, C., Bismuth, G., and Trautmann, A. (1991). Ca^{2+} induced Ca^{2+} release amplifies the Ca^{2+} response elicited by inositol trisphosphate in macrophages. Cell Regul. *2*, 513–522.

Seino, A., Kobayashi, M., Kobayashi, J., Fang, Y., Ishiboshi, M., Nakamura, H., Momose, K., and Ohizumi, Y. (1991). 9-Methyl-7-Bromoudistomin D, a powerful radiolabelable Ca^{2+} releaser having

caffeine-like properties, acts on Ca^{2+}-induced Ca^{2+} release channels of sarcoplasmic reticulum. J. Pharmacol. Exp. Ther. *256*, 861–867.

Smith, J.S., Coronado, R., and Meissner, G. (1986). Single channel measurements of the calcium release channel from skeletal muscle sarcoplasmic reticulum. Activation by Ca^{2+} and ATP and modulation by Mg^{2+}. J. Gen. Physiol. *88*, 573–588.

Takeshima, H., Nishimura, S., Matsumoto, T., Ishida, H., Kangawa, K., Minamino, N., Matsuo, H., Haneoka, M., Hirose, T., and Numa, S. (1989). Primary structure and expression from complementary DNA of skeletal muscle ryanodine receptor. Nature *339*, 439–445.

Thayer, S.A., Hirning, L.D., and Miller, R.J. (1988). The role of caffeine-sensitive stores in the regulation of the intracellular free calcium concentration in rat sympathetic neurons in vitro. J. Pharmacol. Exp. Ther. *34*, 664–673.

Tsunoda, Y. (1991). Oscillatory Ca^{2+} signalling and its cellular function. New Biol. *3*, 3–17.

Verma, A., Hirsch, D.J., Hanley, M.R., Thastrup, O., Christensen, S.B., and Snyder, S.H. (1990a). Inositol trisphosphate and thapsigargin discriminate endoplasmic reticulum stores of calcium in rat brain. Biochem. Biophys. Res. Commun. *172*, 811–816.

Verma, A., Ross, C.A., Verma, D., Supattapone, S., and Snyder, S.H. (1990b). Rat brain endoplasmic reticulum calcium pools are anatomically and functionally segregated. Cell Regul. *1*, 781–790.

Walton, P.D., Airey, J.A., Sutko, J.L., Beck, C.F., Mignery, G.A., Sudhof, T.C., Deerinch, T.J., and Ellisman, M.H. (1991). Ryanodine and inositol trisphosphate receptors co-exist in avian cerebellar Purkinje neurons. J. Cell. Biol. *113*, 1145–1147.

Wimsatt, D.K., Hahl, C.M., Brierley, G.P., and Altschuld, R.A. (1990). Calcium accumulation and release by the sarcoplasmic reticulum of digitonin-lysed adult mammalian ventricular cardiomyocytes. J. Biol. Chem. *265*, 14849–14857.

Worley, P.F., Baraban, J.M., Supattapone, S., Wilson, V.S., and Snyder, S.H. (1987). Characterization of inositol trisphosphate receptor binding in brain: regulation by pH and calcium. J. Biol. Chem. *262*, 12132–12136.

Zimanyi, I., and Pessah, I.N. (1991). Pharmacological characterization of the specific binding of [^{3}H]ryanodine to rat brain microsomal membranes. Brain Res. *561*, 181–191.